Atmos. Chem. Phys. Discuss., 8, 4911–4947, 2008
www.atmos-chem-phys-discuss.net/8/4911/2008/

Atmospheric Chemistry and Physics Discussions

Model simulations of stratospheric ozone loss caused by enhanced mesospheric NO_x during Arctic Winter 2003/2004

B. Vogel[1], P. Konopka[1], J.-U. Grooß[1], R. Müller[1], B. Funke[2], M. Lopéz-Puertas[2], T. Reddmann[3], G. Stiller[3], T. von Clarmann[3], and M. Riese[1]

[1]Research Centre Jülich, Institute for Stratospheric Research (ICG-1), Jülich, Germany
[2]Instituto de Astrofísica de Andalucía, CSIC, Granada, Spain
[3]Forschungszentrum Karlsruhe, Institute for Meteorology and Climate Research, Karlsruhe, Germany

Received: 9 January 2008 – Accepted: 25 January 2008 – Published: 6 March 2008

Correspondence to: B. Vogel (b.vogel@fz-juelich.de)

Published by Copernicus Publications on behalf of the European Geosciences Union.

Abstract

Satellite observations show that the enormous solar proton events (SPEs) in October–November 2003 had significant effects on the composition of the stratosphere and mesosphere in the polar regions. After the October–November 2003 SPEs and in early 2004 significant enhancements of NO_x(=NO+NO_2) in the upper stratosphere and lower mesosphere in the Northern Hemisphere were observed by several satellite instruments. Here we present global full chemistry calculations performed with the CLaMS model to study the impact of mesospheric NO_x intrusions on Arctic polar ozone loss processes in the stratosphere. Several model simulations are preformed with different upper boundary conditions for NO_x at 2000 K potential temperature (≈50 km altitude). In our study we focus on the impact of the non-local production of NO_x which means the downward transport of enhanced NO_x from the mesosphere in the stratosphere. The local production of NO_x in the stratosphere is neglected. Our findings show that intrusions of mesospheric air into the stratosphere, transporting high burdens of NO_x, affect the composition of the Arctic polar region down to about 400 K (≈17 – 18 km). We compare our simulated NO_x and O_3 mixing ratios with satellite observations by ACE-FTS and MIPAS processed at IMK/IAA and derive an upper limit for the ozone loss caused by enhanced mesospheric NO_x. Our findings show that in the Arctic polar vortex (Equivalent Lat.> 70° N) the accumulated column ozone loss between 350 – 2000 K potential temperature (≈14 – 50 km altitude) caused by the SPEs in October–November 2003 in the stratosphere is up to 3.3 DU with an upper limit of 5.5 DU until end of November. Further we found that about 10 DU but lower than 18 DU accumulated ozone loss additionally occurs until end of March 2004 caused by the transport of mesospheric NO_x-rich air in early 2004. In the lower stratosphere (350 – 700 K≈14 – 27 km altitude) the SPEs of October–November 2003 have negligible small impact on ozone loss processes until end of November and the mesospheric NO_x intrusions in early 2004 yield ozone loss about 3.5 DU, but clearly lower than 6.5 DU until end of March. Overall, the non-local production of NO_x is an additional variability to the

existing variations of the ozone loss observed in the Arctic.

1 Introduction

During periods of solar disturbances solar events can affect the concentration of constituents in the middle atmosphere. Protons, electrons, and alpha particles released from the sun are channelled along the Earth's magnetic field and cause ionization, excitation, dissociation, and dissociative ionization of the background constituents when they reach the Earth's atmosphere. Solar disturbances can also lead to solar proton events (SPEs) which are characterized by emission of protons with higher energies. Some of these highly energetic protons can penetrate to the stratosphere, but generally only in the polar regions. In general, the major effects of solar energetic particle precipitation (EPP) and SPEs have been found to significantly increase the production of odd nitrogen NO_y (N, NO, NO_2, NO_3, N_2O_5, HNO_3, HO_2NO_2, $ClONO_2$, and $BrONO_2$) and odd hydrogen HO_x (H, OH, HO_2) (e. g. Crutzen et al., 1975; Jackman et al., 1980; Solomon et al., 1981; López-Puertas et al., 2005a; Verronen et al., 2006). Both NO_y and HO_x play a key role in the ozone balance of the middle atmosphere because they destroy odd oxygen by catalytic cycles. During polar night conditions, NO_y is long lived and can be transported downwards. Therefore, extra NO_y produced in the upper atmosphere could be important to the ozone budget of the lower and middle stratosphere. In contrast enhanced HO_x produced by SPEs in the mesosphere or upper stratosphere is short-lived and therefore only yields short-time ozone decrease.

The fourth largest period of SPEs measured in the past 40 years happened in October–November 2003 (known as the "Halloween sunstrom"), which resulted in ionization effects in the atmosphere down to 30 km altitude near the geomagnetic poles (e. g. Jackman et al., 2005b). An especially vigorous period of high fluxes of energetic protons occurred from 28 – 31 October 2003 and a second maximum was between 2 – 4 November 2003 (Jackman et al., 2005b). Satellite observations of several instruments have shown that these SPEs have significant effects on the composition of

the Arctic stratosphere and mesosphere. After the SPEs, ozone depletion signatures associated with significant enhancements of NO_x (=NO + NO_2) (e. g. Seppälä et al., 2004; López-Puertas et al., 2005a; Rohen et al., 2005), of several NO_y components like HNO_3 or N_2O_5 (e. g. López-Puertas et al., 2005b; Orsolini et al., 2005), and of HO_x (e. g. Degenstein et al., 2005; von Clarmann et al., 2005) in the upper stratosphere and lower mesosphere were observed.

Further, upper stratospheric and mesospheric enhancements of NO_x were observed at high northern latitudes in early 2004 (e. g. López-Puertas et al., 2005a, 2006; Randall et al., 2005) due to downward transport of upper atmospheric NO_x produced throughout the winter by auroral and precipitating electrons (Funke et al., 2007). Results by Randall et al. (2006) confirm that the impact of EPP on the atmosphere are modulated by meteorological conditions; their results suggest that a stronger vortex leads to increasing NO_x values in the stratosphere caused by descent of NO_x-rich air masses from the mesosphere and thermosphere within a well-isolated vortex.

In fact, the dynamic situation of the Arctic winter 2003/2004 was very anomalous. A major warming beginning in late December 2003 led to nearly 2 months of vortex disruption (Manney et al., 2005). The upper stratospheric vortex broke up in late December, but began to recover by early January. In February and March it was the strongest since regular observations began in 1979. The lower stratospheric vortex broke up in late January, split into two fragments on 1 February with the fragments coalesced again by 17 February. Thus the period when the vortex was strong in the upper stratosphere but very small and weak in the lower to middle stratosphere was quite uncommon (Manney et al., 2005). The temperatures in the lower stratosphere were unusually high and temperatures in middle and upper stratosphere were unusually low during and after February 2004. These dynamic disturbances supported the downward transport of NO_x leading to the NO_x enhancements in the upper stratosphere in early 2004.

In addition to this downward transport of NO_x in the lower stratosphere, dynamic disturbances of the vortex also yielded enhanced meridional transport of NO_x-rich as

well as O_3-rich air masses from the subtropics into the polar regions in the lower stratosphere. This effect was discussed by Konopka et al. (2007a) for the winter 2002/2003. They found that the enhanced meridional transport of NO_x also causes ozone loss that can outweigh the halogen-induced ozone loss processes occurring in winter and early spring in the Arctic lower and middle stratosphere.

In this paper, model simulations with the **C**hemical **La**grangian **M**odel of the **S**tratosphere (CLaMS) (McKenna et al., 2002a,b; Konopka et al., 2007b) will be presented. We analyze for the Arctic winter 2003/2004 the long-term impact of enhanced NO_x in the mesosphere caused by the extremely strong SPEs in October–November 2003 and the mesospheric intrusion in early 2004 on stratospheric ozone budget. Here we focus on the impact of enhanced NO_x on ozone loss caused by downward transport from the mesosphere into the stratosphere, whereas enhancements of different NO_y species below 55 km downward to 30 km altitude observed immediately after the SPEs (e. g. López-Puertas et al., 2005b) due to local production of NO_x are not considered.

2 The model study

To study the impact of downward transport of enhanced NO_x in the Arctic winter 2003/2004 on the stratospheric ozone budget, full chemistry studies are performed with the chemical transport model CLaMS (e. g., Konopka et al., 2003; Grooß et al., 2005). The simulations cover the altitude range from 350 – 2000 K potential temperature (≈14–50 km altitude). The horizontal and vertical transport is driven by ECMWF winds and heating/cooling rates derived from a radiation calculation. The mixing procedure uses the mixing parameter as described in Konopka et al. (2004) with a horizontal resolution of 200 km and a vertical resolution increasing from 3 km around 350 K potential temperature to approximately 13 km around 2000 K potential temperature according to the model set up (Konopka et al., 2007b). The halogen, NO_x, and HO_x chemistry mainly based on the current JPL evaluation (Sander et al., 2006) is included. Before the first SPE has occurred, the model is initialized at 4 October 2003 with mainly

MIPAS observations (V3O) from 3–5 October 2003 (CH_4, CO, N_2O, O_3, NO, NO_2, N_2O_5, HNO_3, H_2O, and $ClONO_2$) processed at the Institut für Metereologie und Klimaforschung Karlsruhe (IMK) and at the Instituto de Astrofísica de Andalucía (IAA), Granada, Spain. CFC-11 is provided by L. Hoffmann (Hoffmann et al., 2007). Some species measured by MIPAS are not available over the full model altitude range, therefore these data are interpolated to typical tropospheric and mesospheric values at the lower and upper boundary, respectively. Other species are taken from the HALOE climatology (Grooß and Russell, 2005) (HCl and HF) or from results of a simulation with the Mainz 2-D model (Gidel et al., 1983; Grooß, 1996). For all species the lower boundary conditions at 350 K are taken through the course of the simulation from these initial values.

In the model, the flux of enhanced NO_x from the mesosphere is implemented in form of the upper boundary conditions at 2000 K potential temperature (≈50 km altitude) which are updated every 24 h. The NO_y constituents NO_x, N_2O_5, HNO_3 and the tracers CH_4, CO, H_2O, N_2O, and O_3 are taken from results of a long-term simulation performed with the KASIMA model (Karlsruhe Simulation Model of the middle Atmosphere) (Kouker et al., 1999). In this KASIMA simulation (T. Reddmann, personal communication, 2007), enhanced NO_x concentrations in the mesosphere during disturbed periods have been derived above 55 km from MIPAS observations (provided by the European Space Agency ESA).

In addition to this CLaMS reference model run (referred to as "ref" run) a model simulation without an additional NO_y-entry (this means no NO_x, N_2O_5, and HNO_3) at the upper boundary is performed. Because most NO_y at the upper boundary is NO_x in the following we refer this simulation without an additional NO_x-source at the upper boundary as "no NO_x" run. In addition, to estimate the possible maximum impact of NO_x on stratospheric ozone loss, we derive a maximum NO_x-entry at the upper boundary condition from several satellite measurements of NO and NO_2 by the MIPAS instrument on board the ENVISAT satellite (provided by IMK/IAA) (Fischer et al., 2007), by the HALOE instrument on board the UARS satellite (Russell et al., 1993), and by

the ACE-FTS instrument on board the SCISAT satellite (Bernath et al., 2005). For this we modify the upper boundary conditions derived from KASIMA. For each day at the upper boundary the NO_x mixing ratios for equivalent latitudes greater or equal 60° N are replaced by the maximum NO_x value observed by any satellite instruments within 60° and 90° N at 2000 K potential temperature at that day, respectively, by the maximum NO or NO_2 value if no NO_x measurement exists in this 24 h period. For days where no satellite observations are available we take the maximum NO_x derived by KASIMA at that day. This model simulation is referred to as "max NO_x" run.

3 Model results

To facilitate an analysis of the downward transport in CLaMS a mesospheric tracer (MS) is implemented in the model which is initialized with 100% at the upper boundary and with zero below. During the model simulation this tracer is held constant at the upper and lower boundary with 100% and 0%, respectively. This tracer quantifies the percentage of air originating from the upper boundary at 2000 K potential temperature. Figure 1a shows that the influence of the upper boundary and mesosphere, respectively, extends downward to about 600–700 K potential temperature from February until June 2004, i. e. slightly above the region where halogens typically effectively destroy ozone in the Arctic polar winter. Strong downward transport from the mesosphere down to 900 K (MS=80%) occur at the beginning of January caused by the recovery of the upper vortex in early January. Further, strong transport down to 1000 K (MS=80%) is found at the beginning of March where the vortex was very strong (cf. Sect. 1, Manney et al., 2005). Figure 1b shows that the upper and middle stratospheric temperatures become atypically low during and after February as also reported by Manney et al. (2005). The lower stratospheric temperatures remain extremely high after the major warming. The final warming and the vortex breakup, respectively, occurred not until end of April 2004, this is very late compared to other winters (WMO, 2007). Figure 1c shows clear signatures of enhanced NO_x which start in October 2003 caused by the large SPEs in

October–November 2003 and propagate downwards from 2000 K to about 800 K potential temperature. Further, Fig. 1c shows that model signatures of increased NO_x in February and March due to downward transport of upper atmospheric NO_x produced throughout the winter by auroral and precipitating electrons (Funke et al., 2007) propagate down to approximately 800 K – 900 K until March 2004. Figure 1d shows NO_x without mesospheric NO_x sources as simulated in the "no NO_x" run. Here a typical seasonal variation of NO_x can be seen that is not disturbed by an additional downward transport.

The accumulated chemical ozone change (ΔO_3) shown in Fig. 2c is derived from the difference between the simulated (see Fig. 2a) and passively transported (see Fig. 2b) ozone. It allows to quantify the chemical contribution to ozone change during the winter. From late January on, meridional transport of ozone-rich air from low-latitudes into the polar regions yields high ozone mixing ratios up to 5–6 ppmv between 500–800 K (see Fig. 2b) caused by the vortex disruption in late January and the very weak lower stratospheric vortex during February and March (cf. Sect. 1). Below about 800 K, accumulated ozone loss dominates the ozone evolution during the winter and early spring (see Fig. 2c). Here, about 0.5 ppmv accumulated ozone loss is simulated from December 2003 until February 2004 and about 1.0–2.0 ppmv in March and April 2004. Above about 800 K, accumulated ozone production dominates the ozone evolution during the winter and early spring (see Fig. 2c). The accumulated ozone production is strongest in late February and early March and yields values up to 4 ppmv between 1300–1700 K. Here the accumulated ozone production is increasing because the sunlight is returned after the polar night. Our findings show that above 800 K the impact of highly enhanced NO_x values in the stratosphere due to downward transport from the mesosphere on ozone is small since these NO_x values do not yield accumulated ozone loss like in altitudes below 800 K. Thus, above 800 K, there is ozone production in the descending mesospheric air only counteracted to a certain extent by ozone loss caused by the very high NO_x intrusion from the mesosphere. In the Arctic polar vortex in winter 2002/2003, only small enhancements of NO_x were found in the stratosphere,

but enhanced ozone was found in an intrusion of mesospheric air descending into the lower stratosphere (Müller et al., 2007). The fact that air masses originate from the mesosphere are characterized by enhanced O_3 values is consistent with our simulations showing ozone production in the descending mesospheric air for the Arctic winter 2003/2004.

Besides NO_x-induced ozone loss also halogen-induced and HO_x-induced ozone loss have an important impact on polar ozone loss processes. However, halogen-induced ozone loss plays a minor role during the winter 2003/2004, because the lower stratospheric temperatures are unusually high caused by the vortex disruption in the lower stratosphere at the end of January. An analysis of ECMWF temperature data shows that PSCs could only occur during December 2003 and January 2004 between approximately 400–800 K potential temperatures (see Fig. 3). Limited to this time period the model simulates a small chlorine activation of up to 700 pptv ClO_x (see Fig. 4a). Note that chlorine activation is only confined to the lower part of the region where most ozone depletion occurred in this time period (see Fig. 4b). This is consistent with results by Vogel et al. (2003) and Konopka et al. (2007a), who found that NO_x-induced ozone loss occurs slightly above the region where halogens destroy ozone in the Arctic polar winter. Consequently, the ozone loss between 500–800 K is not only driven by ClO_x chemistry. Above 800 K, the ClO_x altitude profiles have a maximum around 1600 K potential temperature (≈43 km) during sunlight conditions. During polar night conditions the ClO mixing ratios are low in these altitudes (see Fig. 4a). In general, by the absence of PSCs in the middle stratosphere the destruction of ozone is mainly driven by NO_x, whereas HO_x-induced ozone loss plays an important role in the lowermost stratosphere and in the upper stratosphere and mesosphere, respectively.

4 Intercomparison of model results with satellite observations

4.1 NO_x mixing ratios

To compare our simulated NO_x mixing ratios with satellite observations conducted by MIPAS (processed at IMK/IAA; version: V3O_NO_9 and V3O_NO_2_9) and ACE-FTS (V2.2) the model results are interpolated to the locations of the observations. Figure 5 shows the mean deviations of the simulated NO_x mixing ratios from the satellite observations. The mean deviations are calculated for bins with an altitude range of 200 K potential temperature and for equivalent latitudes poleward of 70° N. Figure 5 shows that the reference run (top row) yields lower NO_x mixing ratios than observed by satellites for the upper levels. This effect is still small about −15% in November (−5 ppbv at 1800 K–2000 K) and is increasing to −101% (−17 ppbv at 1600 K–1800 K) and −151% (−19 ppbv at 1800 K–2000 K), respectively, in December. In January, no satellite data are available poleward of 70° N equivalent latitude for these altitudes. In February a deviation of up to −129% (−77 ppbv at 1800 K–2000 K) is found to ACE-FTS measurements. In March the deviation is even up to −398% (−121 ppbv at 1600 K–1800 K) and −379% (−136 ppbv at 1800 K–2000 K) measured by MIPAS and up to −146 % (−76 ppbv at 1600 K–1800 K) and −202% (−129 ppbv at 1800 K–2000 K) measured by ACE-FTS. The underestimation of upper stratospheric NO_x in the reference run during periods of enhanced transport of NO_x-rich air masses from the mesosphere into the stratosphere indicates that the NO_x mixing ratios prescribed at the upper boundary are too low. As shown above, this effect is very small during the SPEs in October–November, but larger a few weeks after the SPEs in December and enormous during the strong mesospheric intrusion in February and March 2004. Thus, during periods of strong downward transport of NO_x from the mesosphere into the stratosphere these deviations are found. This means that in the KASIMA longterm simulations the NO_x mixing ratios are underestimated at around 2000 K potential temperature (≈50 km altitude). These large differences in NO_x between the KASIMA simulations and the MIPAS IMK/IAA observations are mainly due to the fact that in KASIMA NO_2 nighttime mea-

surements provided by ESA are used as proxy for NO_x. In the lower mesosphere, NO and NO_2 are not in steady state. Thus, at the local time of MIPAS nighttime measurements (10 pm) NO is only partially converted to NO_2 via $NO+O_3$. Further, transport of NO from illuminated regions into the polar night region can act faster than photochemical NO losses which leads to a significant NO contribution even during polar night. In consequence, the average NO contribution to NO_x at 55 km depends on the availability of ozone and on the extension of the polar night area. Therefore NO_2 nighttime measurements are clearly a lower boundary for NO_x. Further two retrieval codes are used. For the KASIMA longterm simulations the ESA operational processor (Raspollini et al., 2006) is used because more NO_2 data are available which is essential to perform the simulations. The observations shown in this work are NO_x data provided by the IMK/IAA retrieval code (Funke et al., 2005) which allows in contrast to the ESA operational processor accurate inference of NO_2 volume mixing ratios under consideration of all important non-LTE processes. The findings of a validation study of MIPAS-ENVISAT NO_2 operational data by Wetzel et al. (2007) are that large differences between both retrieval results appear. Especially at higher latitudes above about 50 to 55 km in February and March 2004 the NO_2 values provided by ESA are lower than by IMK/IAA. This is exactly the region where for the KASIMA simulations NO_2 mixing ratios are derived form MIPAS observations. Below this altitude region mean differences between both processors are up to 40% under perturbed polar night conditions in February and March 2004.

To study the impact of the underestimation of NO_x mixing ratios at the upper boundary, we perform sensitivity tests with modified upper boundary conditions. At the upper boundary all NO_x mixing ratios for equivalent latitudes greater or equal 60° N are replaced by the maximum NO_x value derived by the IMK/IAA-MIPAS retrieval code (V3O_NO_9 and V3O_NO_2_9), observed by HALOE (V19) or by ACE-FTS (V2.2) as described in Sect. 2. In general for this "max NO_x" run the simulated NO_x mixing ratios at the upper levels are somewhat higher than the satellite observations (see Fig. 5, bottom row). In February the deviation is up to 51% (154 ppbv at 1600 K–1800 K) and 77%

(163 ppbv at 1800 K–2000 K) and in March only up to −15% (7 ppbv at 1600 K–1800 K) and 5% (33 ppbv at 1800 K–2000 K) measured by MIPAS and up to 38% (107 ppbv at 1600 K–1800 K) and 33% (116 ppbv at 1800 K–2000 K) measured by ACE-FTS. This is because at the upper boundary the NO_x mixing ratios for equivalent latitudes greater or equal 60° N are mainly replaced by the maximum NO_x value observed by satellites at that day (see Sect. 2). Thus for the "max NO_x" run the CLaMS NO_x values are clearly on average higher than the satellite data as expected. Further, significant differences between the mean deviation calculated with IMK/IAA-MIPAS and ACE-FTS observations occur. Since NO_x decays from the vortex center towards the vortex boundary in the reference run while it remains constant in the "max NO_x" run, differences in the spatial NO_x distribution between the reference and the "max NO_x" run are most pronounced in the outer part of the vortex, i.e. the region where ACE-FTS observations were taken. This is because the solar occultation technique is used by ACE-FTS observations and therefore no profiles during polar night conditions can be derived in contrast to the MIPAS measurements. A recently reported validation between MIPAS and ACE-FTS measurements yields a good agreement of the NO_x values in the frame of these exceptional atmospheric conditions in the Artic winter 2003/2004 (Kerzenmacher et al., 2007). Nevertheless the "max NO_x" run represents an upper limit for the additional NO_x-entry at the upper boundary compared to both MIPAS and ACE-FTS observations.

For the MIPAS measurements in the lower and middle stratosphere (below about 45 km) an overall accuracy of about 10–20% is indicated for NO_2 provided by IMK/IAA-MIPAS, but in cases of extremely high NO_2 in the mesosphere, uncertainties in NO_x between 10–30% are derived (Funke et al., 2005).

Further our findings show that the downward transport of enhanced NO_x values at the upper boundary yields a very inhomogeneous spatial distribution of NO_x and O_3 at altitudes below 2000 K which is consistent with satellite observations shown in Fig. 7 for the 18 March 2004. Figure 7 illustrates as discussed before that ACE-FTS and IMK/IAA-MIPAS NO_x at 2000 K are much higher than the CLaMS reference run. On

18 March 2004, the maximum NO_x mixing ratio measured by MIPAS and ACE-FTS is 328 ppbv and 216 ppbv, respectively, at 2000 K. That is a factor of 2–3 higher than the NO_x values simulated by CLaMS reference run for that day. Nevertheless Fig. 7 shows that simulated and observed ozone mixing ratios are in very good agreement for that day. We will discuss this in the next section in more detail. Finally, Fig. 7 shows that an equivalent latitude of 60° N describes very well the areas of enhanced NO_x mixing ratios because the enhancements depends on the downward transport of NO_x which in turn depends on the vortex strength.

To summarize, we compared the results of two model simulations with the observations: the reference run yielding rather lower NO_x mixing ratios than observed and the "max NO_x" run yielding in general clearly higher NO_x mixing ratios and a larger area of enhanced NO_x mixing ratios compared to satellite observations. Thus these two simulations represent a lower and a clear upper limit of the real distribution and absolute values of NO_x within the Arctic polar vortex.

4.2 O_3 mixing ratios

To compare our simulated O_3 mixing ratios with satellite observations conducted by IMK/IAA MIPAS (Version: V3O_O_3_7 until V3O_O_3_9) and ACE-FTS (V2.2 update) (Dupuy, E. et al., 2007) we calculate the mean deviations of the simulated ozone mixing ratios from the satellite observations similar as in Sect. 4.1 for NO_x mixing ratios. A comparison between MIPAS ozone data retrieved with the IMK/IAA procesor with several ground-based, balloon-borne, and satellite instruments for stratospheric ozone yields mean differences of generally ±10% (Steck et al., 2007). A currently reported validation of ozone from ACE-FTS (V2.0 update) with MIPAS ESA ozone found that the O_3 data are within ±10% between 10–42 km altitude, but increase above this range, with ACE-FTS reporting larger volume mixing ratios than MIPAS by up to 40% around 53 km altitude (Cortesi, U. et al, 2007). Figure 6 shows that for October 2003 the simulations and the observations of O_3 agree over all altitudes, as expected because the simulations are initialized with MIPAS observations. From November until March

2004 the simulations and the observations are in very good agreement for the reference run, expect at the upper levels. Here in general the mean deviation at the upper level increases until February up to −45% (−0.9 ppmv, IMK/IAA-MIPAS) and −97% (−1.9 ppmv, ACE-FTS), respectively. However in March 2004 the mean deviation at the upper level is only −10% (−0.08 ppmv, IMK/IAA-MIPAS) and −72% (−1.4 ppmv, ACE-FTS), respectively. The "max NO_x" run yields in general smaller O_3 mixing ratios as in the reference run, because the NO_x-induced ozone loss is higher in the "max NO_x" run. Thus in February and March 2004, where the largest discrepancies between simulated and observed NO_x occur (cf. Sect. 4.1) the simulated O_3 agrees best with the reference run. For these months simulated O_3 values in the "max NO_x" are clearly lower than the satellite observations. Thus the "max NO_x" run is a clear lower limit for O_3 compared to satellite observations. Furthermore, Fig. 6 shows that enhanced NO_x at the upper boundary has an impact of the O_3 mixing ratios over the whole altitude profile (cf. below, Sect. 5). Finally it is shown in Fig. 6 that the ozone mixing ratios at the upper boundary (that is in the KASIMA model) are a bit too low compared to satellite observations.

In general, differences between observations conducted by IMK/IAA-MIPAS or ACE-FTS and the CLaMS simulations are increasing with altitude, but the form of both altitude profiles is very similar. This is consistent with the fact that above approximately 40 km altitude ACE-FTS reporting larger volume mixing ratios than ESA-MIPAS by up to 40% (Cortesi, U. et al, 2007). The length of the error bars in Fig. 6 indicates the variability in the difference between simulated and observed O_3 values.

Summarizing, the comparison between simulated and observed ozone mixing ratios confirm that the "max NO_x" run is a upper limit case which overestimates the strength of the NO_x intrusions at the upper boundary and underestimates the ozone mixing ratios i. e. the O_3 destruction in this model run is too high compared to IMK/IAA-MIPAS and ACE-FTS measurements. Thus, the reference run yields the best agreement with O_3 satellite observations.

5 Ozone loss

To answer the question what is the quantitative influence of the mesospheric NO_x sources on stratospheric ozone loss, CLaMS simulations with and without a mesospheric NO_x source at the upper model boundary are compared. For the reference model run the respective differences of NO_x ($\Delta_{abs}NO_x$) and O_3 ($\Delta_{abs}O_3$) shown in Fig. 8a and b quantify the increase of NO_x and the ozone loss triggered by the intrusion of mesospheric air. The strong enhancements of NO_x in November/December 2003 and in February/March 2004 are clearly visible in Fig. 8a. The highest mean values (70°–90° N equivalent latitude) of additional NO_x are up to approximately 115 ppbv and occur at the upper boundary in March 2004. The spatial distribution between $\Delta_{abs}NO_x$ and $\Delta_{abs}O_3$ correlates fairly well. The strongest impact of enhanced NO_x on O_3 mixing ratios is found in January between 850 K and 1100 K potential temperature. Here as shown before (cf. Sect. 3) a strong downward transport caused by the recovery of the upper vortex occur that cause up to 1 ppmv (28%) lower ozone mixing ratios than in the "no NO_x" run. Further during the period of the very strong upper vortex in February and March 2004 (cf. Sect. 1) our model results show up to 0.6 – 0.7 ppmv (17%) lower O_3 mixing ratios at the end of March 2004 between 1300 K and 1700 K potential temperature. Furthermore, from the beginning of March on a small impact of enhanced NO_x on ozone is found down to 400 K potential temperature (17–18 km altitude).

The enhanced NO_x mixing ratios have also an impact on HO_x. The spatial distribution of the minima and maxima between $\Delta_{abs}O_3$ and $\Delta_{abs}HO_x$ correlates fairly well (not shown here). Up to approximately 150 pptv (112%) lower HO_x mixing rations as in the "no NO_x" run are found in January between 850 K and 1100 K potential temperature. That means the HO_x-induced ozone loss is lower in the reference run than in the "no NO_x" run.

The impact of mesospheric NO_x sources on the column ozone is shown in Fig. 9a (top panel) integrated over the entire simulated altitude range (≈14–50 km). The column ozone is shown in red for the reference model simulation ("ref"), in blue for the

simulation without mesospheric sources ("no NO_x"), and in yellow for the run with a maximum NO_x source ("max NO_x"). The corresponding accumulated column ozone loss in the stratosphere calculated from the simulated O_3 values minus the passively transported ozone (as shown in Fig. 2) is shown in Fig. 9a (middle panel). Until the end of April a column ozone loss of up to approximately 80 DU is simulated for the reference run and up to approximately 90 DU for the "max NO_x" run. Thereafter the column ozone loss is strongly decreasing because the final warming occurred at the end of April 2004 resulting in transport of midlatitude air masses to the pole that have encountered less chemical ozone depletion. In Fig. 9a (bottom panel) the ozone loss attributed to enhanced mesospheric NO_x intrusion are shown. This value is calculated from the difference between the "no NO_x" run and the reference run (red) and the "max NO_x" run (yellow), respectively. At the end of March the ozone loss attributable to mesospheric NO_x intrusion in early 2004 is up to 10 DU (equivalent to ≈3% of the ozone column) for the reference run and up to 18 DU (equivalent to ≈6% of the ozone column) for the "max NO_xrun (see Fig. 9a, bottom panel). That means that nearly twice the ozone loss occurs in the "max NO_x" run as for the reference run. Further Fig. 9a (bottom panel) shows ΔO_3 of approximately 19 DU at the end of May. This is after the final warming occurred at the end of April. This feature shows that enhanced mesospheric NO_x values have still an impact on ozone chemistry also during the change from polar winter to summer conditions. Thus we conclude that the column ozone loss in the stratosphere at the end of March assigned to mesospheric NO_x sources is about 10 DU but lower than 18 DU. The column ozone loss caused by the SPEs in October–November 2003 in the stratosphere is up to 3.3 DU with an upper limit of 5.5 DU in mid-November. These absolute values are small compared to the ozone loss in spring 2004 caused by the mesospheric NO_x intrusions, but their fraction at the total accumulated ozone loss occurred until mid-November is up to 36% and 48%, respectively.

The presented column ozone loss in the stratosphere is derived for equivalent latitudes greater 70° N. The impact of mesospheric enhanced NO_x is strongest for high equivalent latitudes because the downward transport depends on the vortex strength.

Therefore choosing a wider latitude range to analyze the average column ozone loss yields lower column ozone loss.

Further we also calculate the ozone loss over the winter and the ozone loss caused by mesospheric NO_x sources for the lower stratosphere over an altitude range from 350 K until 700 K (≈14–27 km, see Fig. 9b). Here a total ozone loss until end of April up to 68 DU for the "ref" run and up to 71 DU for the "max NOx" run are found. A maximum column ozone loss at the end of April assigned to mesospheric NO_x sources is up to 3.5 DU for the reference run and 6.5 DU for the "max NO_x" run, respectively. Unfortunately no analyses to the polar stratospheric ozone loss for the Arctic winter 2003/2004 exist so far because the halogen-induced ozone loss plays a minor role and yield very low ozone loss over the winter as mentioned before. But a three-dimensional model study of the Arctic ozone loss in that winter results in an O_3 change of approximately 50 DU between 345–670 K (poleward of 65° equivalent latitude) until end of March and beginning of April (Feng et al., 2005). Our simulations yield 45–50 DU ("ref" run) and 47–52 DU ("max NO_x" run) until end of March and beginning of April. However the simulation by Feng et al. (2005) are started at the beginning of December 2003 and our simulations are started at beginning of October 2003 and second our analysis is for equivalent latitudes poleward of 70° in contrast to 65° in the Feng et al. (2005) study. Nevertheless, we can conclude that our simulations are the same range as the results by Feng et al. (2005). Thus our finding shows that the impact of enhanced mesospheric NO_x values on ozone loss processes in the lower stratosphere (350–700 K) is about 5% but lower than 9% for the Arctic winter 2003/2004.

For cold Arctic winters an accumulated ozone loss in the lower stratosphere was derived in the range of about 100 DU (e. g. Rex et al., 2004; Tilmes et al., 2006). Thus in cold Arctic winters with strong halogen-induced ozone loss the impact on the column ozone of enhanced mesospheric NO_x values as analyzed in this work would be very small. Moreover Fig. 9b (bottom panel) shows that first from Mid-February during the period of the very strong upper stratospheric vortex enhanced mesospheric NO_x values have an impact on ozone loss below 700 K. Thus in the lower stratosphere (350–700 K)

the non-local production of NO_x caused by SPEs of October–November 2003 have a negligibly small impact on ozone loss.

In our simulations the enhancements of different NO_y species below 55 km downward to 30 km altitude observed immediately after the SPEs (e. g. López-Puertas et al., 2005b) caused by particle precipitation reaching the stratosphere are not considered. The impact of local NO_x production on polar ozone loss is considered in a study by Jackman et al. (2005a), where the influences of all the solar proton fluxes between 2000 and 2003 with a 2-D CTM is simulated. They found an impact on total ozone of 0.5–3% (≈2–10 DU) (WMO, 2007), whereas we derive a column ozone loss about 2.5 DU, but lower than 4.5 DU caused by the October–November 2003 SPEs. Taking into account that we neglect the local NO_x production below 55 km in October–November 2003 in our model simulations and only consider the downward transport of enhanced NO_x it is not surprising that our results are at the lower limit of the predictions by Jackman et al. (2005a).

6 Summary and conclusions

The impact of downward transport of enhanced upper atmospheric NO_x caused by solar proton events in October–November 2003 and by mesospheric NO_x intrusions in early 2004 produced throughout the winter by auroral and precipitating electrons on the stratospheric ozone budget was studied performing model simulations with the chemical transport model CLaMS. Upper boundary conditions were taken from results of a longterm simulation conducted with KASIMA, where increased NO_x concentration in the mesosphere have been derived from MIPAS measurements (reference run). For the Arctic polar region (Equivalent Lat. >70° N) we found that enhanced NO_x caused by SPEs in October–November 2003 is transported downward into the middle stratosphere to about 800 K potential temperature (≈30 km) until end of December 2003. The mesospheric NO_x intrusion due to downward transport of upper atmospheric NO_x produced by auroral and precipitating electrons (Funke et al., 2007) affects NO_x mix-

ing ratios down to about 700 K potential temperature (≈27 km) until March 2004. A comparison of the reference run with a simulation without an additional NO_x source at the upper boundary show that O_3 mixing ratios are affected by transporting high burdens of NO_x down to about 400 K (≈17–18 km) during the winter. Locally, an additional ozone loss of the order 1 ppmv is simulated for January between 850–1200 K potential temperature during the period of the strong polar vortex in the middle stratosphere. We point out that the enhancements of different NO_y species below 55 km downward to 30 km altitude due to local production of NO_x observed immediately after the SPEs (e. g. López-Puertas et al., 2005b) caused by particle precipitation down in the stratosphere are not considered in our simulations as well as the local production of HO_x. Thus in our simulations only the non-local production of NO_x, namely the transport of enhanced NO_x from the mesosphere (upper boundary condition) to the stratosphere is considered and the local production of NO_x and HO_x is neglected.

An intercomparison of simulated NO_x and O_3 mixing ratios with satellite observations by ACE-FTS and MIPAS shows that the NO_x mixing ratios at the upper boundary derived from KASIMA simulations are in general too low. Therefore a model simulation with higher NO_x mixing ratios at the upper boundary derived from satellite measurements was performed. For this model run ("max NO_x") the simulated NO_x mixing ratios and the total area of enhanced NO_x mixing ratios are in general higher compared to satellite observations and provide so an upper limit for the impact of mesospheric NO_x on stratospheric ozone chemistry. The comparison between simulated and observed ozone mixing ratios confirm the "max NO_x" run is an upper limit which overestimates the NO_x entry at the upper boundary and underestimates O_3 caused due to stronger O_3 destruction. Moreover in the "ref" run the simulated O_3 is in very good agreement with satellite measurements.

Our findings show that halogen-induced ozone loss plays a minor role in the Arctic winter 2003/2004 because the lower stratospheric temperatures were unusually high. Therefore the ozone loss processes in the Arctic winter stratosphere 2003/2004 are mainly driven by NO_x chemistry. Further, in addition to the transport of NO_x-rich meso-

spheric air masses in the stratosphere due to SPEs in October–November 2003 and the downward transport of upper atmospheric NO_x produced by auroral and precipitating electrons in early 2004, the ozone loss processes are also strongly affected by meridional transport of subtropical air masses. Likewise, in this case air masses rich in both ozone and NO_x are transported during the major warming occurred in December 2003 and January 2004 into the lower polar stratosphere.

We found that up to 80 DU total ozone loss occurred in the stratosphere until end of April 2004 between 350–2000 K potential temperature (≈14–50 km). The additional ozone loss caused by transport of mesospheric NO_x-rich air into the stratosphere is about 10 DU (3%) but lower than 18 DU (6%) found end of March 2004. Due to the SPEs of the Halloween sunstorm event an additional accumulated ozone loss of approximately 3.3 DU (36%) but below 5.5 DU (48%) was simulated until mid-November 2003. Thus the absolute impact on total accumulated ozone loss of the mesospheric NO_x intrusion in early 2004 is stronger as of the SPEs in October–November 2003, but the relative impact is smaller. In the lower stratosphere (350–700 K ≈14–27 km) the non-local production of NO_x caused by SPEs of October–November 2003 have negligible small impact on ozone loss until end of November and the mesospheric NO_x intrusions in early 2004 yield small ozone loss about 3.5 DU (5%), but lower than 6.5 DU (9%) until end of March. Thus, owing to the meteorological conditions, NO_x enhancements caused by the mesospheric NO_x intrusion in early 2004 have a stronger impact on ozone loss processes in the lower stratosphere than the enhanced NO_x values caused by October–November SPEs. Because the strength of the upper stratospheric vortex after the major warming in early 2004 is stronger than for the vortex in late 2003, the downward transport of enhanced NO_x form the mesosphere down in the lower stratosphere in early 2004 is more effective.

Acknowledgements. The authors are grateful to Martin Kaufmann for initiating this project. We thank J. M. Russell III (Hampton University) for providing the HALOE V19 data and the scientific team of ACE-FTS for providing the ACE-FTS data. The Atmospheric Chemistry Experiment (ACE), also known as SCISAT, is mainly supported by the Canadian Space Agency.

ACE-FTS data were kindly provided by ESA-ESRIN as Third Party Mission (TPM) data. MIPAS level-1b and level-2 data were provided by ESA. The IAA team was supported by the Spanish project ESP2004-01556 and EC FEDER funds. Our activities were funded by the German Science Foundation (Deutsche Forschungsgemeinschaft, DFG) in the framework of the project "**C**limate **a**nd **W**eather of the **S**un-**E**arth **S**ytem (CAWSES)" within the subproject "**M**iddle **A**tmosphere **NO**$_x$ variations and solar **U**V **Va**riability (MANOXUVA): Examples to study mesospheric/stratospheric coupling and the impact of solar variability on stratospheric ozone" under contract number KO 2958/1-1.

References

Bernath, P., McElroy, C., Abrams, M., et al.: Atmospheric Chemistry Experiment (ACE): Mission overview, Geophys. Res. Lett., 32, L15S01, doi:10.1029/2005GL022386, 2005. 4917

Cortesi, U., Lambert, C., De Clercq, G., et al.: Geophysical validation of MIPAS-ENVISAT operational ozone data, Atmos. Chem. Phys., 7, 4807–4867, 2007. 4923, 4924

Crutzen, P. J., Isaksen, I. A. S., and Reid, G. C.: Solar proton events: Stratospheric sources of nitric oxide, Science, 189, 457–459, 1975. 4913

Degenstein, D. A., Lloyd, N. D., Bourassa, A. E., Gattinger, R. L., and Llewellyn, E. J.: Observations of Mesospheric Ozone Depletion during the October 28, 2003 Solar Proton Event by OSIRIS, Geophys. Res. Lett., 32, L03S11, doi:10.1029/2004GL021521, 2005. 4914

Dupuy, E., Walker, K. A., Kar, J., et al.: Validation of ozone measurements from the Atmospheric Chemistry Experiment (ACE), Atmos. Chem. Phys. Discuss., 8, 2513–2656, 2008, http://www.atmos-chem-phys-discuss.net/8/2513/2008/. 4923

Feng, W., Chipperfield, M. P., Davies, S., Sen, B., Toon, G., Blavier, J. F., Webster, C. R., Volk, C. M., Ulanovsky, A., Ravegnani, F., von der Gathen, P., Jost, H., Richard, E. C., and Claude, H.: Three-dimensional model study of the Arctic ozone loss in 2002/2003 and comparison with 1999/2000 and 2003/2004, Atmos. Chem. Phys., 5, 139–152, 2005. 4927

Fischer, H., Birk, M., Blom, C., et al.: MIPAS: An instrument for atmospheric and climate research, Atmos. Chem. Phys. Discuss., 7, 8795–8893, 2007, http://www.atmos-chem-phys-discuss.net/7/8795/2007/. 4916

Funke, B., von Clarmann, M. L.-P. T., Stiller, G. P., Fischer, H., Glatthor, N., Grabowski, U., Höpfner, M., Kellmann, S., Kiefer, M., Linden, A., Tsidu, G. M., Milz, M., Steck, T., and Wang,

D. Y.: Retrieval of stratospheric NO_x from 5.3 and 6.2 μm nonlocal thermodynamic equilibrium emissions measured by Michelson Interferometer for Passive Atmospheric Sounding (MIPAS) on Envisat, J. Geophys. Res., 110, D09302, doi:10.1029/2004JD005225, 2005. 4921, 4922

Funke, B., López-Puertas, M., Fischer, H., Stiller, G., von Clarmann, T., Wetzel, G., Carli, B., and Belotti, C.: Comment on "Origin of the January–April 2004 increase in stratospheric NO_2 observed in northern polar latitudes" by Jean-Baptist Renard et al., Geophys. Res. Lett., 34, l07813, doi:10.1029/2006GL027518, 2007. 4914, 4918, 4928

Gidel, L. T., Crutzen, P. J., and Fishman, J.: A two-dimensional photochemical model of the atmosphere; 1: Chlorocarbon emissions and their effect on stratospheric ozone, J. Geophys. Res., 88, 6622–6640, 1983. 4916

Grooß, J.-U.: Modelling of Stratospheric Chemistry based on HALOE/UARS Satellite Data, PhD thesis, University of Mainz, 1996. 4916

Grooß, J.-U. and Russell, J. M.: Technical note: A stratospheric climatology for O_3, H_2O, CH_4, NO_x, HCl, and HF derived from HALOE measurements, Atmos. Chem. Phys., 5, 2797–2807, 2005. 4916

Grooß, J.-U., Günther, G., Müller, R., Konopka, P., Bausch, S., Schlager, H., Voigt, C., Volk, C. M., and Toon, G. C.: Simulation of denitrification and ozone loss for the Arctic winter 2002/2003, Atmos. Chem. Phys., 5, 1437–1448, 2005. 4915

Hoffmann, L., Kaufmann, M., Spang, R., Müller, R., Volk, C. M., and Riese, M.: Envisat MIPAS measurements of CFC-11: Retrieval, Validation, and Climatology, Atmos. Chem. Phys. Discuss., accepted, 2007. 4916

Jackman, C. H., Frederick, J. E., and Stolarski, R. S.: Production of odd nitrogen in the stratosphere and mesophere – an intercomparison of source strengths, J. Geophys. Res., 85(NC12), 7495–7505, 1980. 4913

Jackman, C. H., DeLand, M. T., Labow, G. J., Fleming, E. L., Weisenstein, D. K., Ko, M. K. W., Sinnhuber, M., Anderson, J., and Russell, J. M.: The influence of the several very large solar proton events in years 2000–2003 on the neutral middle atmosphere, Adv. Space Res., 35, 445–450, 2005a. 4928

Jackman, C. H., DeLand, M. T., Labow, G. J., Fleming, E. L., Weisenstein, D. K., Ko, M. K. W., Sinnhuber, M., and Russell, J. M.: Neutral atmospheric influences of the solar proton events in October–November 2003, J. Geophys. Res., 110, A09S27, doi:10.1029/2004JA010888, 2005b. 4913

Kerzenmacher, T., Wolff, M. A., Strong, K., et al.: Validation of NO_2 and NO from Atmospheric Chemistry Experiment (ACE), Atmos. Chem. Phys. Discuss., 8, 3027–3142, 2008 4922

Konopka, P., Grooß, J.-U., Bausch, S., Müller, R., McKenna, D. S., Morgenstern, O., and Orsolini, Y.: Dynamics and chemistry of vortex remnants in late Arctic spring 1997 and 2000: Simulations with the Chemical Lagrangian Model of the Stratosphere (CLaMS), Atmos. Chem. Phys., 3, 839–849, 2003, http://www.atmos-chem-phys.net/3/839/2003/. 4915

Konopka, P., Steinhorst, H.-M., Grooß, J.-U., Günther, G., Müller, R., Elkins, J. W., Jost, H.-J., Richard, E., Schmidt, U., Toon, G., and McKenna, D. S.: Mixing and Ozone Loss in the 1999–2000 Arctic Vortex: Simulations with the 3-dimensional Chemical Lagrangian Model of the Stratosphere (CLaMS), J. Geophys. Res., 109, D02315, doi:10.1029/2003JD003792, 2004. 4915

Konopka, P., Engel, A., Funke, B., Müller, R., Grooß, J.-U., Günther, G., Wetter, T., Stiller, G., von Clarmann, T., Glatthor, N., Oelhaf, H., Wetzel, G., López-Puertas, M., Pirre, M., Huret, N., and Riese, M.: Ozone loss driven by nitrogen oxides and triggered by stratospheric warmings may outweigh the effect of halogens, J. Geophys. Res., 112, D05105, doi:10.1029/2006JD007064, 2007a. 4915, 4919

Konopka, P., Günther, G., Müller, R., Santos, F. H., Schiller, C., Ravegnani, F., Ulanovsky, A., Schlager, H., Volk, C. M., Viciani, S., Pan, L., McKenna, D. S., and Riese, M.: Contribution of mixing to upward transport across the tropical tropopause layer (TTL), Atmos. Chem. Phys., 7, 12, 3285–3308, 2007b. 4915

Kouker, W., Langbein, I., Reddmann, T., and Ruhnke, R.: The Karlsruhe Simulation Model of the Middle Atmosphere (KASIMA), Version 2, Wissenschaftliche Berichte FZKA 6278, Forschungszentrum Karlsruhe, 1999. 4916

López-Puertas, M., Funke, B., Gil-López, S., von Clarmann, T., Stiller, G. P., Höpfner, M., Kellmann, S., Fischer, H., and Jackman, C. H.: Observation of NO_x enhancement and ozone depletion in the Northern and Southern hemispheres after the October–November 2003 Solar Proton Events, J. Geophys. Res., 110, A09S43, doi:10.1029/2005JA011050, 2005a. 4913, 4914

López-Puertas, M., Funke, B., Gil-López, S., von Clarmann, T., Stiller, G. P., Höpfner, M., Kellmann, S., Mengistu Tsidu, G., Fischer, H., and Jackman, C. H.: HNO_3, N_2O_5 and $ClONO_2$ Enhancements after the October–November 2003 Solar Proton Events, J. Geophys. Res., 110, A9, doi:10.1029/2005JA011051, 2005b. 4914, 4915, 4928, 4929

López-Puertas, M., Funke, B., Clarmann, T., Fischer, H., and Stiller, G.: The Variability of

Stratospheric and Mesospheric NO_y in the Arctic and Antarctic 2002–2004 Polar Winters, Space Sci. Rev., 125, 403–416, doi:10.1007/s11214-006-9073-2, 2006. 4914

Manney, G. L., Krüger, K., Sabutis, J. L., Amina Sena, S., and Pawson, S.: The remarkable 2003-2004 winter and other recent warm winters in the Arctic stratosphere in the late 1990s, J. Geophys. Res., 110, D04107, doi:10.1029/2004JD005367, 2005. 4914, 4917

McKenna, D. S., Grooß, J.-U., Günther, G., Konopka, P., Müller, R., Carver, G., and Sasano, Y.: A new Chemical Lagrangian Model of the Stratosphere (CLaMS): 2. Formulation of chemistry scheme and initialization, J. Geophys. Res., 107, D15, 4256, doi:10.1029/2000JD000113, 2002a. 4915

McKenna, D. S., Konopka, P., Grooß, J.-U., Günther, G., Müller, R., Spang, R., Offermann, D., and Orsolini, Y.: A new Chemical Lagrangian Model of the Stratosphere (CLaMS): 1. Formulation of advection and mixing, J. Geophys. Res., 107, D16, 4309, doi:10.1029/2000JD000114, 2002b. 4915

Müller, R., Tilmes, S., Grooß, J.-U., Engel, A., Oelhaf, H., Wetzel, G., Huret, N., Pirre, M., Catoire, V., Toon, G., and Nakajima, H.: Impact of mesospheric intrusions on ozone–tracer relations in the stratospheric polar vortex, J. Geophys. Res., 112, D23307, doi:10.1029/2006JD008315, 2007. 4919

Orsolini, Y. J., Manney, G., Santee, M., and Randall, C.: An upper stratospheric layer of enhanced HNO_3 following exceptional solar storms, Geophys. Res. Lett., 32, 12, L12S01, doi:10.1029/2004GL021588, 2005. 4914

Randall, C. E., Harvey, V. L., Manney, G. L., Orsolini, Y., Codrescu, M., Sioris, C., Brohede, S., Haley, C. S., Gordley, L. L., Zawodny, J. M., and Russell, J. M.: Stratospheric effects of energetic particle precipitation in 2003–2004, Geophys. Res. Lett., 32, 5, L05802, doi:10.1029/2004GL022003, 2005. 4914

Randall, C. E., Harvey, V. L., Singleton, C. S., Bernath, P. F., Boone, C. D., and Kozyra, J. U.: Enhanced NO_x in 2006 linked to strong upper stratospheric Arctic vortex, Geophys. Res. Lett., L18811, doi:10.1029/2006GL027160, 2006. 4914

Raspollini, P., Belotti, C., Burgess, A., Carli, B., Carlotti, M., Ceccherini, S., Dinelli, B. M., Dudhia, A., Flaud, J.-M., Funke, B., Höpfner, M., López-Puertas, M., Payne, V., Piccolo, C., Remedios, J. J., Ridolfi, M., and Spang, R.: MIPAS level 2 operational analysis, Atmos. Chem. Phys., 6, 5605–5630, 2006. 4921

Rex, M., Salawitch, R. J., von der Gathen, P., Harris, N. R. P., Chipperfield, M. P., and Naujokat, B.: Arctic ozone loss and climate change, Geophys. Res. Lett., 31, L04116, doi:10.1029/

2003GL018844, 2004. 4927
Rohen, G., von Savigny, C., Sinnhuber, M., Llewellyn, E. J., Kaiser, J. W., Jackman, C. H., Kallenrode, M.-B., Schröter, J., Eichmann, K.-U., Bovensmann, H., and Burrows, J. P.: Ozone depletion during the solar proton events of October/November 2003 as seen by SCIAMACHY, J. Geophys. Res., 110, A09S39, doi:10.1029/2004JA010984, 2005. 4914
Russell, J. M., Gordley, L. L., Park, J. H., Drayson, S. R., Tuck, A. F., Harries, J. E., Cicerone, R. J., Crutzen, P. J., and Frederick, J. E.: The Halogen Occultation Experiment, J. Geophys. Res., 98, 10 777–10 797, 1993. 4916
Sander, S. P., Friedl, R. R., Golden, D. M., Kurylo, M. J., Huie, R. E., Orkin, V. L., Moortgat, G. K., Wine, P. H., Ravishankara, A. R., Kolb, C. E., Molina, M. J., and Finlayson-Pitts, B. J.: Evaluation number 15, Chemical kinetics and photochemical data for use in atmospheric studies, NASA Panel for Data Evaluation, JPL Publication 06-2, Jet Propulsion Laboratory, California Insitute of Technology, Pasadena, California, 2006. 4915
Seppälä, A., Verronen, P., Kyrölä, E., Hassinen, S., Backman, L., Hauchecorne, A., Bertaux, J., and Fussen, D.: Solar proton events of October–November 2003: Ozone depletion in the Northern Hemisphere polar winter as seen by GOMOS/Envisat, Geophys. Res. Lett., 31, (L19107), doi:10.1029/2004GL021042, 2004. 4914
Solomon, S., Rusch, D. W., J. C. GERARD, G. C. R., and Crutzen, P. J.: The effect of particle precipitation events on the neutral and ion chemistry of the middle atmosphere: II. Odd hydrogen, Planet. Space Sci., 29, 8, 885–892, 1981. 4913
Steck, T., von Clarmann, T., Fischer, H., Funke, B., Glatthor, N., Grabowski, U., Höpfner, M., Kellmann, S., Kiefer, M., Linden, A., Milz, M., Stiller, G. P., Wang, D. Y., Allaart, M., Blumenstock, T., von der Gathen, P., Hansen, G., Hase, F., Hochschild, G., Kopp, G., Kyrö, E., Oelhaf, H., Raffalski, U., Marrero, A. R., Remsberg, E., III, J. R., Stebel, K., Steinbrecht, W., Wetzel, G., Yela, M., , and Zhang, G.: Bias determination and precision validation of ozone profiles from MIPAS-Envisat retrieved with the IMK-IAA processor, Atmos. Chem. Phys., 7, 3639–3662, 2007, http://www.atmos-chem-phys.net/7/3639/2007/. 4923
Tilmes, S., Müller, R., Grooß, J.-U., and Russell, J. M.: Ozone loss and chlorine activation in the Arctic winters 1991–2003 derived with the tracer-tracer correlations, Atmos. Chem. Phys., 4, 8, 2181–2213, 2004. 4939
Tilmes, S., Müller, R., Engel, A., Rex, M., and Russell III, J.: Chemical ozone loss in the Arctic and Antarctic stratosphere between 1992 and 2005, Geophys. Res. Lett., 33, L20812, doi: 10.1029/2006GL026925, 2006. 4927

Verronen, P. T., Seppälä, A., Kyrölä, E., Tamminen, J., Pickett, H. M., and Turunen, E.: Production of odd hydrogen in the mesosphere during the January 2005 solar proton event, Geophys. Res. Lett., 33, 24, doi:10.1029/2006GL028115, L24811, 2006. 4913

Vogel, B., Müller, R., Deshler, T., Grooß, J.-U., Karhu, J., McKenna, D. S., Müller, M., Toohey, D., Toon, G. C., and Stroh, F.: Vertical profiles of activated ClO and ozone loss in the Arctic vortex in January and March 2000: In situ observations and model simulations, J. Geophys. Res., 108, D22, 8334, doi:10.1029/2002JD002564, 2003. 4919

von Clarmann, T., Glatthor, N., Höpfner, M., Kellmann, S., Ruhnke, R., Stiller, G. P., Fischer, H., Funke, B., Gil-López, S., and López-Puertas, M.: Experimental Evidence of Perturbed Odd Hydrogen and Chlorine Chemistry After the October 2003 Solar Proton Events, J. Geophys. Res., 110, A9, doi:10.1029/2005JA011053, 2005. 4914

Wetzel, G., Bracher, A., Funke, B., Goutail, F., Hendrick, F., Lambert, J.-C., Mikuteit, S., Piccolo, C., Pirre, M., Bazureau, A., Belotti, C., Blumenstock, T., De Maziere, M., Fischer, H., Huret, N., Ionov, D., López-Puertas, M., Maucher, G., Oelhaf, H., Pommereau, J.-P., Ruhnke, R., Sinnhuber, M., Stiller, G., Van Roozendael, M., and Zhang, G.: Validation of MIPAS-ENVISAT NO_2 operational data, Atmos. Chem. Phys., 7, 3261–3284, 2007, http://www.atmos-chem-phys.net/7/3261/2007/. 4921

WMO: Scientific assessment of ozone depletion: 2006, Global Ozone Research and Monitoring Project-Report No. 50, Geneva, Switzerland, 2007. 4917, 4928

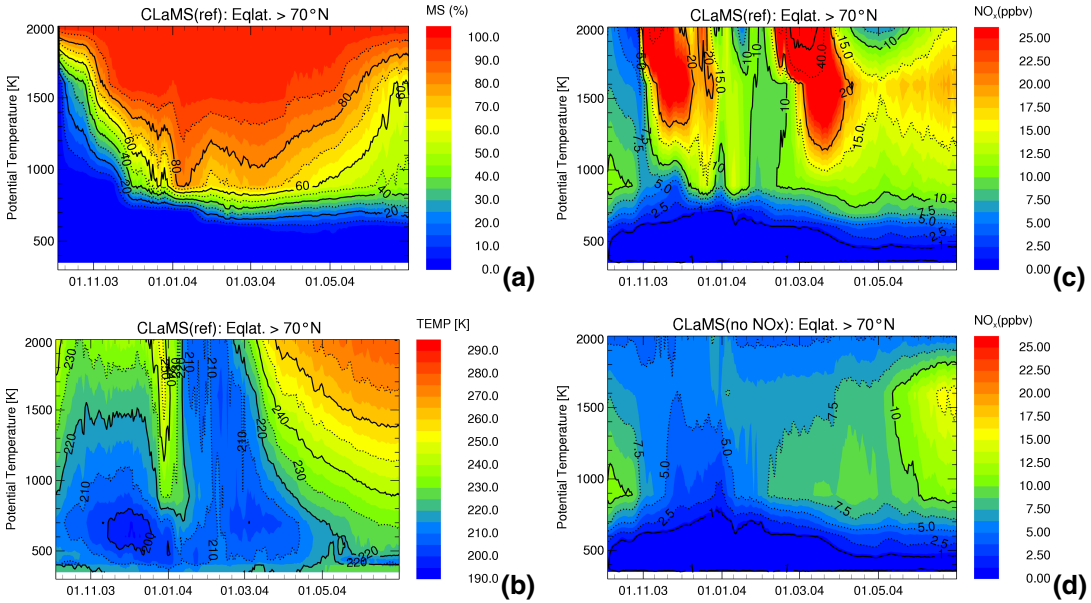

Fig. 1. Mean distributions, poleward of 70° N equivalent latitude, of **(a)** the mesospheric tracer MS, **(b)** the temperature, **(c)** NO_x (=NO+NO_2) for the reference model run ("ref") and **(d)** for a simulation without an addition NO_x source at the upper boundary ("no NO_x"). To compare panel c) and d) the color range are the same, but in panel c) the maximum NO_x mixing ratios are much higher than the color range (see isolines). The potential temperature range from 350 to 2000 K corresponds to ≈14 to 50 km altitude.

ACPD
8, 4911–4947, 2008

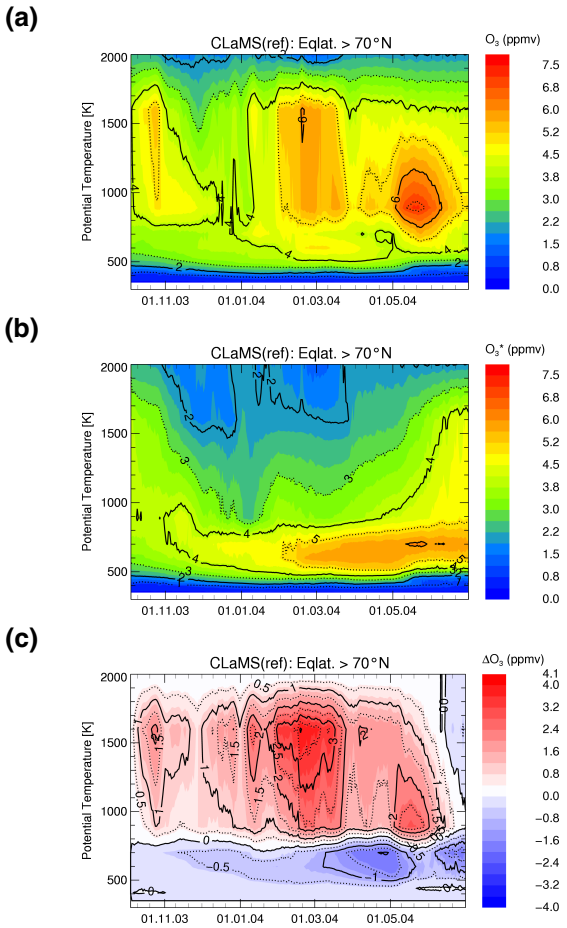

Fig. 2. Mean distributions, poleward of 70° N equivalent latitude, of **(a)** ozone, **(b)** passively transported ozone (O_3*), and **(c)** the accumulated chemical ozone change ($\Delta O_3 = O_3 - O_3$*) from the reference simulation performed with CLaMS.

ACPD
8, 4911–4947, 2008

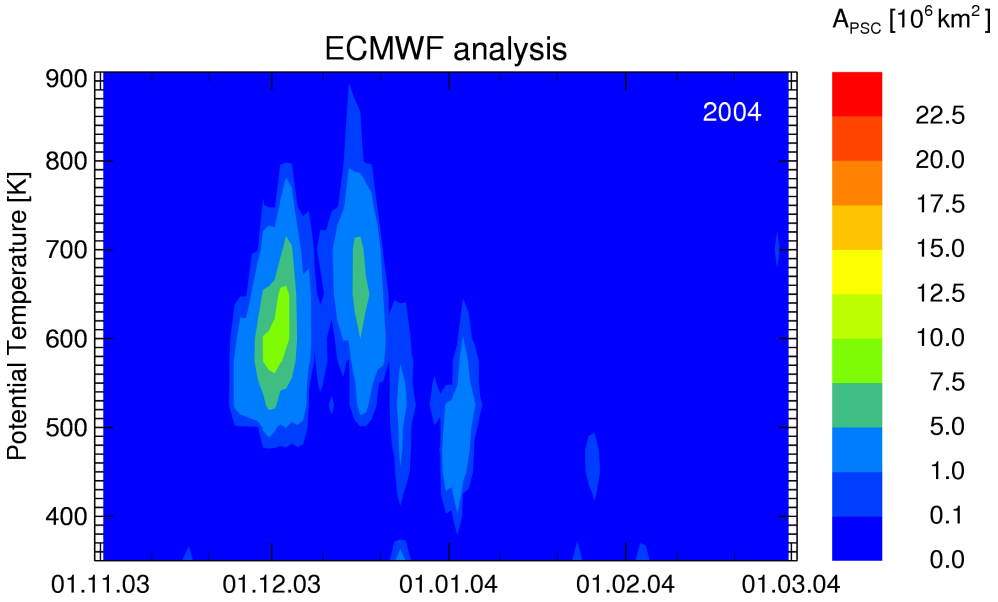

Fig. 3. Time series of the areas of potential PSC occurrence (A_{PSC}) derived from ECMWF temperatures and T_{NAT} estimate. The color code indicates that the A_{PSC} are very small compared to cold Arctic winter where A_{PSC} up to 22×10^6 km^2 can occur (Tilmes et al., 2004).

ACPD
8, 4911–4947, 2008

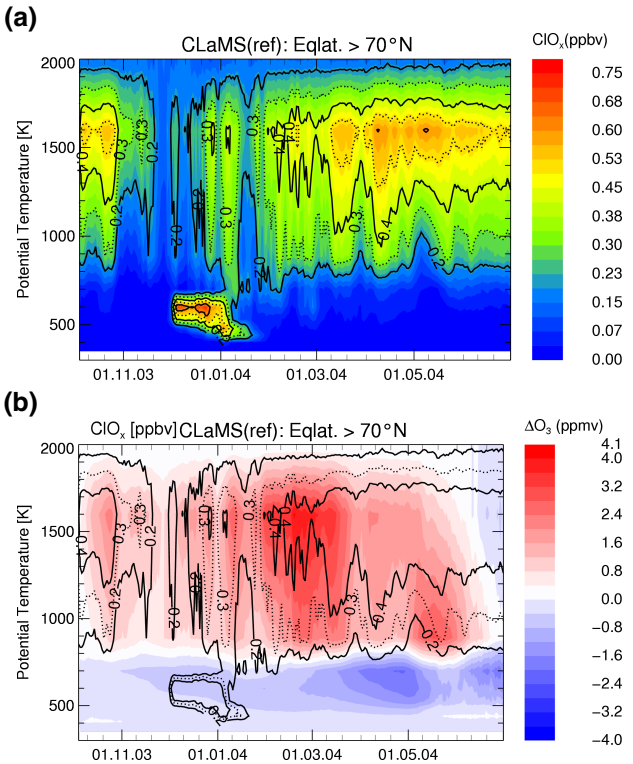

Fig. 4. **(a)** Time series of the mean distribution of activated chlorine ($ClO_x = ClO + 2 \times Cl_2O_2$) poleward of 70° equivalent latitude for the reference model run. Panel **(b)** shows the chemical ozone change same as Fig. 2**c**, but with contour lines of the mean distribution of ClO_x. It is clearly shown that the region of chlorine activation caused by PSC occurrence is mainly in the lower part of the region where most ozone loss occurred at that time.

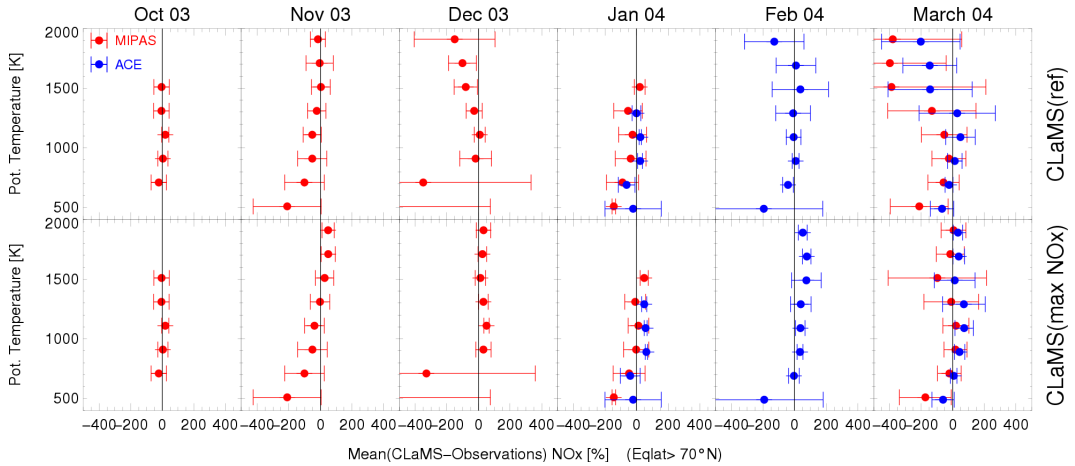

Fig. 5. The mean deviations of the simulated NO_x mixing ratios from MIPAS observations processed at IMK/IAA (red) and from ACE-FTS observations (blue, from January 2004). The mean deviations are calculated for bins with an altitude range of 200 K potential temperature and for equivalent latitudes poleward of 70° N. In the columns, the mean deviations from October 2003 until March 2004 are shown. In the top row the results for the reference run and in the bottom row the "max NO_x" run are shown. The standard deviation of the mean deviations is indicated by error bars. We note that for February 2004 no NO_x data from MIPAS processed at IMK/IAA are available. The plot symbols are shifted by a small range in y-direction to distinguish better between MIPAS and ACE-FTS observations.

ACPD
8, 4911–4947, 2008

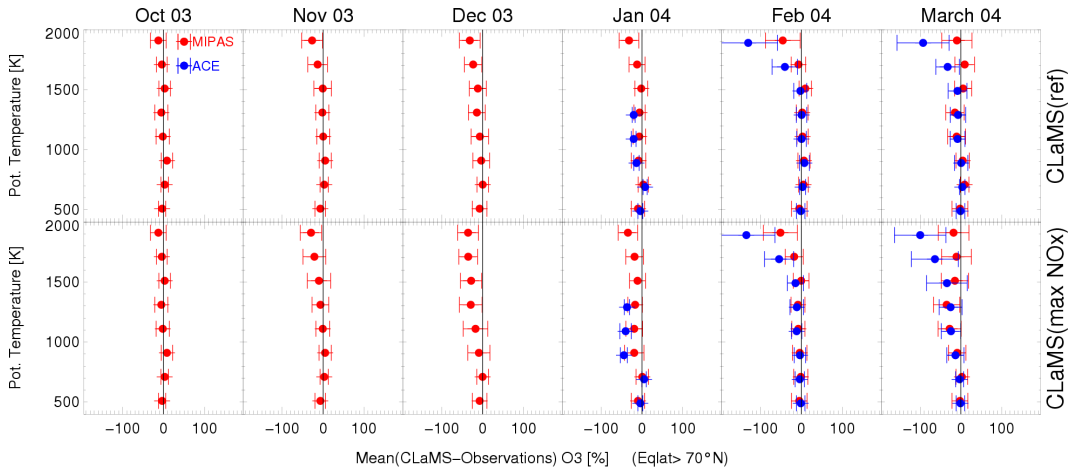

Fig. 6. As Fig. 5, but for ozone.

ACPD
8, 4911–4947, 2008

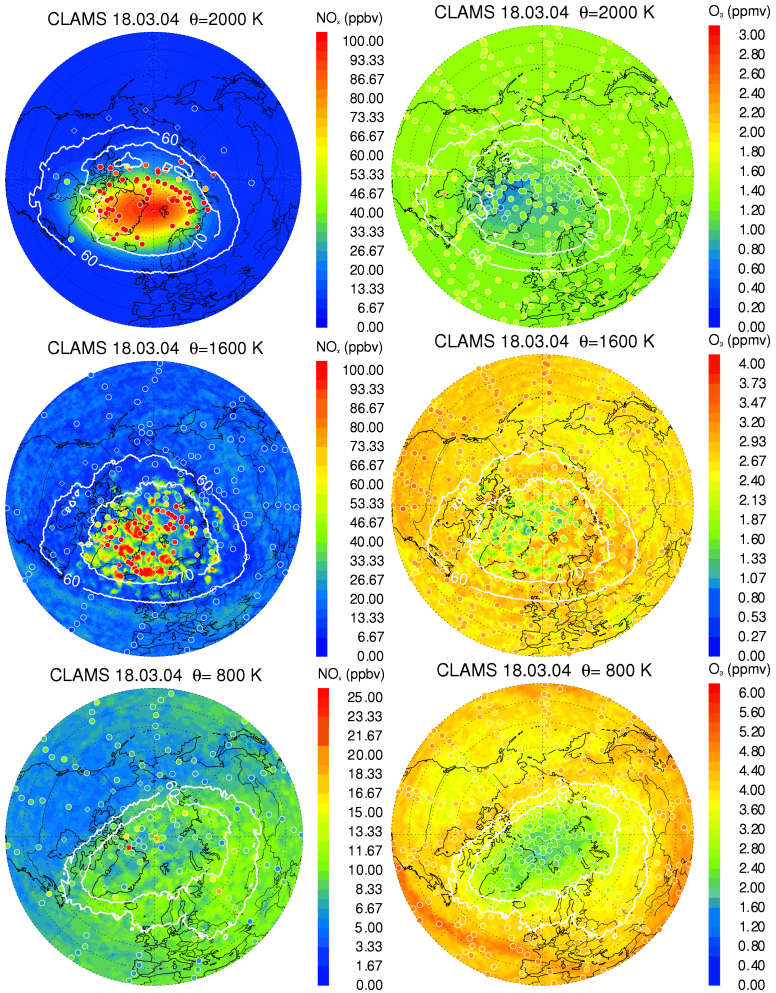
CLAMS 18.03.04 θ=2000 K
NOx (ppbv)
100.00
93.33
86.67
80.00
73.33
66.67
60.00
53.33
46.67
40.00
33.33
26.67
20.00
13.33
6.67
0.00
CLAMS 18.03.04 θ=2000 K
O3 (ppmv)
3.00
2.80
2.60
2.40
2.20
2.00
1.80
1.60
1.40
1.20
1.00
0.80
0.60
0.40
0.20
0.00
CLAMS 18.03.04 θ=1600 K
NOx (ppbv)
100.00
93.33
86.67
80.00
73.33
66.67
60.00
53.33
46.67
40.00
33.33
26.67
20.00
13.33
6.67
0.00
CLAMS 18.03.04 θ=1600 K
O3 (ppmv)
4.00
3.73
3.47
3.20
2.93
2.67
2.40
2.13
1.87
1.60
1.33
1.07
0.80
0.53
0.27
0.00
CLAMS 18.03.04 θ= 800 K
NOx (ppbv)
25.00
23.33
21.67
20.00
18.33
16.67
15.00
13.33
11.67
10.00
8.33
6.67
5.00
3.33
1.67
0.00
CLAMS 18.03.04 θ= 800 K
O3 (ppmv)
6.00
5.60
5.20
4.80
4.40
4.00
3.60
3.20
2.80
2.40
2.00
1.60
1.20
0.80
0.40
0.00

Fig. 7.

Fig. 7. Horizontal view of NO_x and O_3 at 2000 K, 1600 K, and 800 K potential temperature for the reference model run. The isolines for the equivalent latitude at 60° N and 70° N are marked by white lines. The model results and satellite observations (IMK/IAA-MIPAS: circles and ACE-FTS: diamonds) are shown for noon time. We note that all NO_x mixing ratios beyond the scale are also plotted in red.

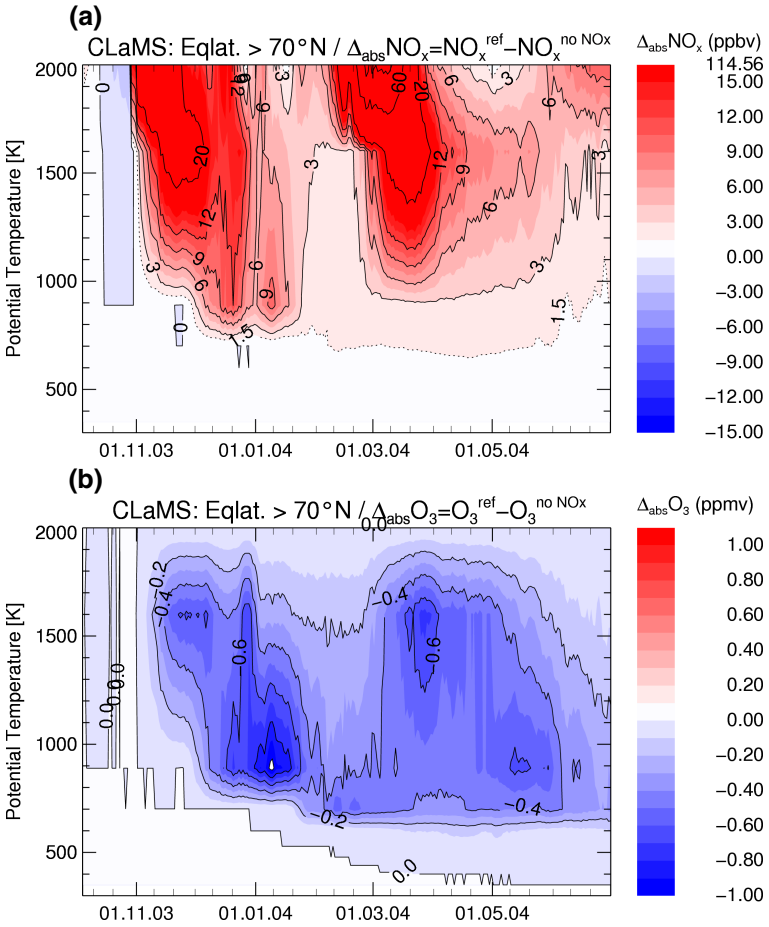

Fig. 8. (a) Additional NO_x ($\Delta_{abs}NO_x$) and **(b)** ozone reduction $\Delta_{abs}O_3$ poleward of 70° N equivalent latitude due to mesospheric NO_x intrusions over the course of the winter 2003–2004 for the reference model run.

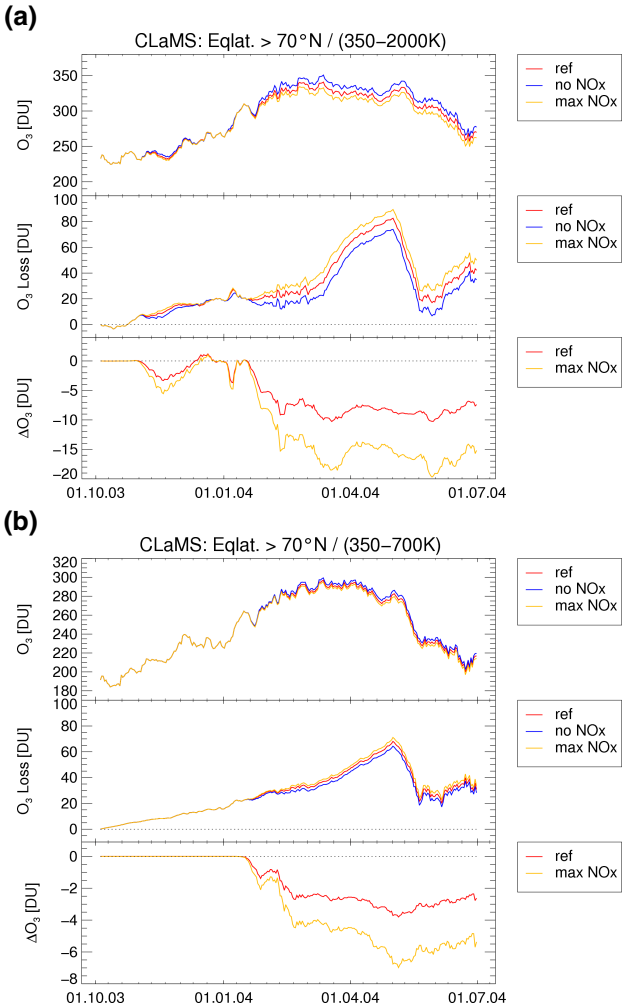

Fig. 9.

ACPD
8, 4911–4947, 2008

Fig. 9. **(a)** Top panel: Column ozone (in Dobson units) with (red), without (blue), and with a maximum (yellow) mesospheric NO_x sources integrated over the entire simulated altitude range from 350 K until 2000 K (≈14–50 km) for equivalent latitudes poleward of 70° N. Middle panel: Ozone loss in DU for these model runs. Bottom panel: ΔO_3 caused by the addition NO_x-source at the upper boundary. Shown is the ozone column of the "no NO_x" run minus the ozone column of the "ref" (red) and the "max NO_x" run (yellow). **(b)** same as (a), but for an altitude range from 350 K until 700 K (≈14–27 km) potential temperature.